



Imaging of thymic epithelial tumors—a clinical practice review

Sho Koyasu[^]

Department of Diagnostic Imaging and Nuclear Medicine, Graduate School of Medicine, Kyoto University, Kyoto, Japan

Correspondence to: Sho Koyasu, MD, PhD. Department of Diagnostic Imaging and Nuclear Medicine, Graduate School of Medicine, Kyoto University, 54 Shogoin Kawahara-cho, Sakyo-ku, Kyoto 606-8507, Japan. Email: sho@kuhp.kyoto-u.ac.jp.

Abstract: This review article comprehensively examines the diagnostic approach to thymic epithelial tumors (TETs) and other mediastinal masses, focusing on imaging modalities and differential diagnosis. Beginning with a discussion on traditional and contemporary classification systems for mediastinal tumors, including the Japanese Association for Research on the Thymus (JART) and International Thymic Interest Group (ITMIG) classifications, it highlights the shift towards computed tomography (CT)-based categorizations. Emphasis is placed on the importance of distinguishing between solid and cystic lesions in the anterior mediastinum, with detailed insights into imaging characteristics and histological features of various TET subtypes such as thymomas, thymic carcinomas, and thymic neuroendocrine tumors (NETs). The review also elucidates common differential diagnoses, including lymphomas and germ cell tumors, providing guidance on key imaging findings and considerations for accurate diagnosis. Furthermore, it underscores the significance of patient background and blood tests in differential diagnosis, discussing age-related prevalence patterns and tumor marker assessment. After addressing the diagnostic challenges posed by thymic cysts offering insights into their radiological features, management considerations, and potential complications, this review extends to other rare mediastinal lesions highlighting the need for a comprehensive evaluation for accurate identification and management of these tumors. Finally, as illustrative examples, we present six cases highlighting various aspects of anterior mediastinal tumors, including TET. These cases provide valuable insights into the diagnostic challenges, imaging characteristics, and management considerations encountered in clinical practice. The cases presented herein do not all illustrate typical images, courses, and diagnoses. However, they each contain significant implications. Thus, we present them with the belief that they will aid in understanding the intricate nuances of image diagnosis in actual clinical practice.

Keywords: Computed tomography (CT); magnetic resonance imaging (MRI); thymoma; thymic carcinoma; thymic epithelial tumor (TET)

Received: 06 December 2023; Accepted: 16 May 2024; Published online: 07 June 2024.

doi: 10.21037/med-23-66

View this article at: <https://dx.doi.org/10.21037/med-23-66>

Introduction

Thymic epithelial tumors (TETs) represent a major subset of mediastinal tumors, located in the central compartment of the thoracic cavity known as the mediastinum. The mediastinum encompasses important structures such as the heart, major arteries and veins, esophagus, trachea, lymphatics and thymus, giving rise to a diverse series of

potential neoplastic entities collectively termed mediastinal tumors. The complexity of mediastinal tumors demands a meticulous approach to differential diagnosis.

Traditionally, the classification of mediastinal tumors relied on classical mediastinal divisions derived from lateral chest radiographs or Felson's mediastinal classifications (1). However, the year 2009 marked a pivotal development with

[^] ORCID: 0000-0002-6690-7460.

the introduction of the Japanese Association for Research on the Thymus (JART) classification, which utilized computed tomography (CT) cross-sectional images to categorize mediastinum (2). Subsequently, the International Thymic Interest Group (ITMIG) further streamlined the JART classification into the ITMIG classification, simplifying the approach to mediastinal tumor localization (3-5).

The primary distinction between the JART and ITMIG classifications lies in the definition of the superior mediastinum. Specifically, JART maintains the traditional concept of the superior mediastinum, whereas ITMIG opts for a more streamlined approach, categorizing the entire mediastinum into only three segments: the anterior, middle, and posterior mediastinum. The ITMIG classification opts for a three-compartment model for defining mediastinal compartments due to its simplicity and anatomical accuracy, despite potential limitations in adequately separating entities occurring in different locations. The four-compartment model, while offering similarity to existing models and potential effectiveness in distinguishing disease entities, suffers from complexity and non-anatomic boundaries. Concerns were raised about the artificial division between superior and inferior compartments, which may allow the spread of infectious, inflammatory processes, and tumors without restriction by fascial planes, and the lack of adherence by posterior neurogenic tumors to this division. Thus, experts' preference for the three-compartment model, citing reasons such as optimal distinction of diseases, familiarity, anatomical accuracy, and ease of use, led to its selection as the basis for the proposed CT-based classification scheme by ITMIG (3).

As conventionally recognized, the upper mediastinum harbors thyroid lesions, the middle mediastinum encompasses cystic lesions such as bronchogenic cysts, and the posterior mediastinum is associated with a higher incidence of neurogenic tumors.

This review focuses on TET, the majority of which manifest in the anterior mediastinum. However, tumors that occur in this region are not limited to TET, but range from malignant lymphoma to germ cell tumors. The differential diagnosis of TET, especially in the pre-diagnostic phase of imaging, can be aided by a combination of imaging and blood tests including tumor markers.

The aim of this review is to present comprehensive information on the imaging diagnosis of TET, the most frequent solid tumors arising in the anterior mediastinum, as well as other rare tumors of the anterior mediastinum among others.

Diagnostic approach of TETs

Tumors arising in the thymus are of various histological types, but three types of TET are the most frequent: thymomas, thymic carcinomas, and thymic neuroendocrine tumors (NETs) (6). Regardless of these subtypes, the initial step in the diagnostic process involves distinguishing between solid and cystic lesions. This is crucial as anterior mediastinal masses, including TET, often require differentiation from conditions such as pericardial cysts and thymic cysts, which are common cystic lesions in the anterior mediastinum. Contrast-enhanced CT proves invaluable in this context, with a post-contrast enhancement of generally 20 Hounsfield units (HU) or more indicative of a solid lesion. Conversely, 10–15 HU change in attenuation can be due to various non-specific factors, such as incorrect placement of the region of interest, patient motion, or beam hardening from adjacent enhancing structures (7). There may be high rate of unnecessary thymectomy due to misinterpretation of thymic cysts, thymic hyperplasia, and lymphoma as thymoma on chest CT. A recent study showed that differentiating features between thymoma, lymphoma, thymic hyperplasia, and thymic cysts on chest CT which may help triage more patients away from thymectomy toward less invasive and non-invasive means of diagnosis and thereby lower the non-therapeutic thymectomy rate (8). In instances where CT-based differentiation is challenging, T2-weighted images (T2WI), showing marked high signal intensity and high apparent diffusion coefficient (ADC) values, can suggest cystic lesions, whereas the absence of these features increases the likelihood of a solid lesion (9,10).

The subsequent step involves considering and ruling out other solid tumors occurring in the anterior mediastinum. The common differential diagnoses include lymphomas and germ cell tumors. When lymphomas arise in the mediastinum, three prevalent subtypes—Hodgkin lymphoma, primary mediastinal large B-cell lymphoma, and T-lymphoblastic lymphoma—are frequently encountered. Shared characteristics among these lymphomas include a propensity to progress without directly invading or encasing existing blood vessels, while calcification is infrequent (11,12). However, distinctions arise in terms of necrosis; Hodgkin lymphoma exhibits a lower frequency of necrosis, while the other subtypes often present with pronounced necrosis, resulting in heterogeneous internal structures. Additionally, these two lymphomas may lead to complications such as pleural effusion or pericardial effusion (11). In addition, as mentioned earlier, the

common finding in lymphoma is a penetrating image of blood vessels. Lymphomas exhibit less desmoplastic change compared to solid tumors. In cases of lung or thymic epithelia tumors, during the infiltration process, there may be strong compression of blood vessels or direct infiltration leading to occlusion or severe stenosis. However, such imaging changes are less common in lymphomas, serving as a distinguishing feature from solid tumors. Additionally, in lymphomas (especially Hodgkin lymphoma), which develops multicentrically it is not uncommon for vessels to be surrounded. Nevertheless, even in such instances, relatively minimal stenosis is observed, sometimes resembling blood vessels penetrating the tumor interior, which can be considered a characteristic imaging feature of lymphomas. However, since the venous pressure is lower than that of arteries, stenosis or obstruction of superior vena cava (SVC) or innominate vein is rather common especially non-Hodgkin lymphoma (21%) (13). When a patient presents with SVC syndrome, we should be careful not to assume that lymphoma is ruled out only because of the presence of vascular compression. Ultrasound is a non-invasive and cost-effective imaging modality that can potentially be used to diagnose thymic lesions. Although ultrasound has some limitations in evaluating the entire thymus or thymic lesions especially when they are large, the thymus is reported to be visible in ultrasound examination in all age groups from the suprasternal view in children. Thymus or thymic tumors often extend upward to the cervical area or located in the neck (more common in younger patients), thus ultrasound may be a great help to distinguish cystic and solid lesions (14-16), or there might be a chance of early detection of incidental thymic lesions when observed during thyroid sonography.

Germ cell tumors are categorized into seminomas and non-seminomas. Seminomas typically present with relatively homogeneous internal structures and rare calcifications. In contrast, non-seminomatous germ cell tumors often manifest with internal heterogeneity, frequently accompanied by necrosis or hemorrhage, and may show calcifications (17). Notably, choriocarcinomas within non-seminomatous germ cell tumors can produce human chorionic gonadotropin (hCG), leading to gynecomastia in young males (18). Teratomas, characterized by the presence of diverse tissues, may exhibit features such as mixed fat and calcifications (19). It is well known that some cases of teratoma of the anterior mediastinum are detected by chest pain due to cyst wall disruption (20). It has also been reported that the inclusion of pancreatic tissue is associated

with the risk of wall disruption (21).

Patient background and blood tests serve as valuable considerations in the differential diagnosis of these anterior mediastinal tumors. TET, including thymomas, often afflict individuals in the fifth and sixth decades of life (patient age range, 6–83 years; median: 58 years overall, but 48 years in the black population), and are exceedingly rare in children (6), while malignant lymphomas and germ cell tumors frequently occur in younger individuals (below 40 years) (22). Blood tests measuring tumor markers such as anti-acetylcholine receptor antibodies, complete blood count, gamma globulin, alpha-fetoprotein (AFP), beta-hCG (β -HCG), lactate dehydrogenase (LDH), and soluble interleukin-2 receptor (sIL-2R) aid in the differentiation (23). Thymomas, for instance, may exhibit positive anti-acetylcholine receptor antibodies, making it desirable to include their measurement as a screening tool for concurrent myasthenia gravis (24). Thymomas are also associated with conditions like pure red cell aplasia and hypogammaglobulinemia (Good syndrome), emphasizing the importance of checking complete blood count and globulin (25). In germ cell tumors, elevated levels of AFP, β -HCG, and LDH are common, while malignant lymphomas often present with elevated LDH and sIL-2R. Additionally, it is crucial not to overlook the possibility of primary lung cancer (or lesions associated with lung cancer), a frequent occurrence in mediastinal masses. Therefore, before categorizing a mediastinal mass as a thymic tumor, it is prudent to consider possibilities such as carcinoembryonic antigen (CEA), cytokeratin fragment (CYFRA), and progastrin-releasing peptide (ProGRP) measurements.

With these considerations in mind, the subsequent sections will elaborate on general aspects and imaging diagnostics of TET, including thymomas, thymic carcinomas, and thymic NETs. In addition to these TET, it is also pertinent to mention thymic cysts (cystic lesions) at the end of this section.

Thymoma

Thymoma, the most common anterior mediastinal tumor, predominantly manifests in middle-aged individuals (range, 55–65 years) and is infrequent in children. Gender predilection is not observed. Often asymptomatic, it is frequently incidentally discovered through imaging studies. Thymoma is associated with various autoimmune disorders, with severe myasthenia gravis occurring in 17–54% of cases as mentioned above (6). The prevalences of myasthenia gravis are also reported to vary by ethnicity, with some

reports ranging from 5.7–82.4% (26).

Tumors are histologically classified into types A, AB, B1, B2, and B3 based on the morphology of tumor epithelial cells and the extent of lymphocyte infiltration. This classification correlates with prognosis, where types A to B3 show an increasing frequency of extracapsular invasion and poorer outcomes. Types A, AB, and B1 are considered low-risk, while B2 and B3 are high-risk. The Masaoka staging system, demonstrating a strong correlation between prognosis and clinical stage, is widely used (27). In contrast to thymic carcinoma, thymoma is often misunderstood as a benign tumor. However, its International Classification of Diseases for Oncology (ICD-O) coding ending in 3 classifies it as a potentially malignant lesion. We should recognize every thymoma has potential for metastasis to diverse sites, including the liver, muscles, ovaries, bones, central nervous system, and kidneys (28-31).

Imaging findings of thymoma include distinctive features depending on the histological type. Low-risk thymomas appear as well-circumscribed, smoothly contoured, circular masses with visible capsules and internal septa. They exhibit homogeneous enhancement, with minimal invasion into surrounding structures (32,33). Conversely, high-risk (B2/B3) thymomas often demonstrate irregular shapes with heterogeneous contrast enhancement. Margins are often lobulated, and may include cystic degeneration, necrosis, and hemorrhage, contributing to a tendency for uneven contrast enhancement. Excluding hemorrhagic or cystic components, ADC, which is commonly calculated using magnetic resonance imaging (MRI) with at least two diffusion-weighted imaging (DWI) with different b values, tends to be lower in high-risk thymomas than in low-risk counterparts (34). Although fluorodeoxyglucose-positron emission tomography-CT (FDG PET-CT) is not routinely used for TET, the maximum standardized uptake values (SUV_{max}) of high- and low-risk thymomas were significantly lower than those of thymic carcinomas (35). It also reported that B3 thymomas and thymic carcinomas tend to exhibit higher FDG uptake compared to low-risk thymomas (36).

Although distant metastasis and lymph node involvement are infrequent, thymomas often lead to pleural dissemination. Differential diagnosis may be challenging, particularly with thymic hyperplasia. In cases where CT findings seems inconclusive, MRI with chemical shift imaging becomes valuable, especially if fat components are present, suggesting the possibility of hyperplasia (37).

Thymic carcinoma

Thymic carcinoma, constituting 14–22% of TET, demonstrates a lower incidence compared to thymomas. Patients with thymic carcinoma often manifest symptoms related to mediastinal mass lesions, with high frequencies of invasion into surrounding organs, lymph node metastases, and distant metastases, resulting in a poor prognosis. Paraneoplastic syndromes that are commonly present in patients with thymoma are very rare (38). Imaging findings typically show irregular margins, presenting as irregular or lobulated forms, with cystic degeneration, hemorrhage, and necrosis observed inside the tumor. The distinction from thymic carcinoma and high-risk thymomas on imaging can be challenging, but thymic carcinoma tends to exhibit internal heterogeneity and higher rates of infiltration into the surrounding structures, along with increased frequency of distant metastases (32). Specific patterns on imaging, such as low T2 signal intensity in cases of squamous cell carcinoma (39) and evident calcifications in mucinous carcinoma (40), may support the diagnosis of carcinoma. In terms of the association between the volume-dependent parameters in FDG PET/CT and clinical prognosis, the metabolic tumor volume and total lesion glycolysis may be predictive of the postoperative recurrence of thymic carcinoma (41).

Carcinoid/NET of the thymus

NET arising from the thymus, characterized by the dominance or near-total presence of neuroendocrine cells in TET, account for 2–5% of TET. Most occur in adult patients. All thymic neuroendocrine neoplasms (NENs), which includes both NET and neuroendocrine carcinomas, share a propensity for recurrence, lymph node or distant metastasis, and tumor-associated death, with increasing risk from low-grade to high-grade tumors (42). Their radiological appearance is basically indistinguishable from that of thymic carcinomas (43). These tumors, classified into atypical carcinoids and typical carcinoids, often exhibit large, irregularly margined masses without distinct capsules on imaging. The internal signal and contrast effects on T2WI tend to be heterogeneous. The assessment of ADC values can be challenging due to necrosis and cystic degeneration. Atypical carcinoids, which are defined as having higher mitoses than typical carcinoids and/or having foci of necrosis, in particular, frequently display local

invasion and difficulty in differentiation on imaging, but the presence of abundant hemorrhagic components with a mesh-like septum internally may be indicative of this condition. Feeder vessels may also be identified on contrast-enhanced CT (44).

In the diagnostic imaging of NENs, the utility of nuclear medicine examinations utilizing somatostatin receptor (SSTR) expression, such as SSTR-single photon emission CT (SSTR-SPECT) and SSTR-PET, has recently been recognized. SSTRs, primarily SSTR2, have been identified in a subset of NETs and carcinomas. For instance, DOTATATE and DOTATOC are clinically available somatostatin analogues that bind to SSTR2. These agents can be linked to radionuclides like ^{68}Ga -DOTATATE PET scans correlated with SSTR2 expression in TET in most patients and appeared to be useful to identify patients with TET who may be amenable to treatment with somatostatin analogues (45). There are also reports of using SSTR-PET for the assessment of treatment response in TET (46). However, it is important to note that accumulation does not necessarily indicate NENs and may also be observed in squamous cell carcinomas and thymomas (45).

Thymic cysts (cystic lesions)

Thymic cysts occur within or arise from the thymus gland mainly in anterior mediastinum or rarely in other mediastinal compartment. They can be congenital or acquired, and may be associated with thymic tumors, inflammatory processes, or immunodeficiency. They are usually asymptomatic, but may cause cough, dyspnea, or chest pain if large or complicated. Thymic cysts can be diagnosed by their radiological features, such as unilocular or multilocular cystic masses with well-defined walls, lobulated shape, and variable attenuation depending on the presence of hemorrhage or infection. Thymic cysts are different from TET (thymomas, thymic carcinomas, and thymic NETs as above), which are solid neoplasms that may show heterogeneous enhancement, necrosis, invasion, or calcification. However, thymic cysts are often misinterpreted as solid lesions such as thymic epithelial neoplasms only by CT, or sometimes even by MRI because thymic cysts often showed features suggestive of intralesional microbleeding, inflammation, and fibrosis (47). Recent study describes that most thymic cysts changed in volume [31 of 34 cysts (91%)], CT attenuation [15 of 35 cysts (43%)], and T1-weighted

MRI signal [12 of 18 cysts (67%)] over more than 5 years of follow-up, although none developed mural irregularity, nodularity, or septations (48). The treatment for thymic cysts depends on the size, location, and association with other diseases. Pure thymic cysts are considered benign and may not require any intervention if they are small and asymptomatic. However, some authors recommend surgical resection to confirm the diagnosis and prevent complications. Video-assisted thoracic surgery (VATS) is a reliable and minimally invasive approach for the surgical resection of thymic cysts.

Cases

Case 1

A female in her forties was incidentally identified with abnormalities during a health check-up, with no elevated tumor markers (AFP, CYFRA, CEA, NSE, SCC, SLX, GRP, and anti-AChR antibody: within normal limit). Chest X-ray revealed a protruding mediastinal mass on the left side with the hilum overlay sign (*Figure 1A*). A plain CT showed calcifications (*Figure 1B*, arrow). A contrast-enhanced CT showed intratumoral septal enhancement (*Figure 1C*, arrow). A low signal septum was seen in the same location on T2-weighted MRI (*Figure 1D*, arrow). FDG-PET/CT revealed intense FDG uptake (*Figure 1E*). Overall, the image findings were suggestive of a high-risk thymoma. The patient underwent anterior mediastinal tumor (thymus) resection, which revealed a partially calcified and hemorrhagic mass. Histologically, it was diagnosed as a B3-type thymoma (60% B3, 40% B2) with invasion into the mediastinal pleura. There was no lymph node metastasis and the staging was pT1b pN0 [Union for International Cancer Control (UICC) 8], Masaoka-Koga: IIb.

Case 2

A male patient in his fifties, without any noteworthy medical history, was diagnosed with numerous liver neoplasms during a regular health check-up abdominal ultrasound. A CT scan with contrast revealed ill-defined low-density lesions in the liver and a nodule in the anterior mediastinum (*Figure 2*). The liver biopsy revealed a diffuse proliferation of small to medium-sized T lymphocytes, implying T-lymphoblastic lymphoma/leukemia with terminal deoxynucleotidyl transferase (TdT) positivity. However, due to the presence of a mediastinal nodule and

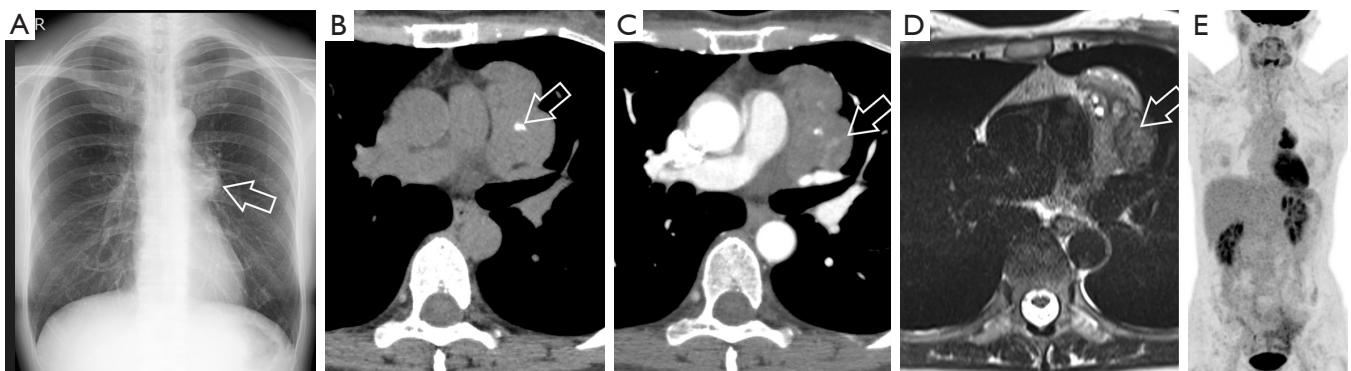


Figure 1 Case 1: a female in her forties was incidentally identified with abnormalities during a health check-up, with no elevated tumor markers. (A) Chest X-ray; (B) plain CT (axial); (C) contrast-enhanced CT (axial); (D) T2WI (axial); (E) FDG-PET (MIP). Chest X-ray revealed a protruding mediastinal mass on the left side with the hilum overlay sign (A, arrow). A plain CT showed calcifications (B, arrow). A contrast-enhanced CT showed intratumoral septal enhancement (C, arrow). A low signal septum was seen in the same location on T2-weighted MRI (D, arrow). FDG-PET/CT revealed intense FDG uptake. CT, computed tomography; T2WI, T2-weighted images; FDG, fluorodeoxyglucose; PET, positron emission tomography; MIP, maximum intensity projection; MRI, magnetic resonance imaging.

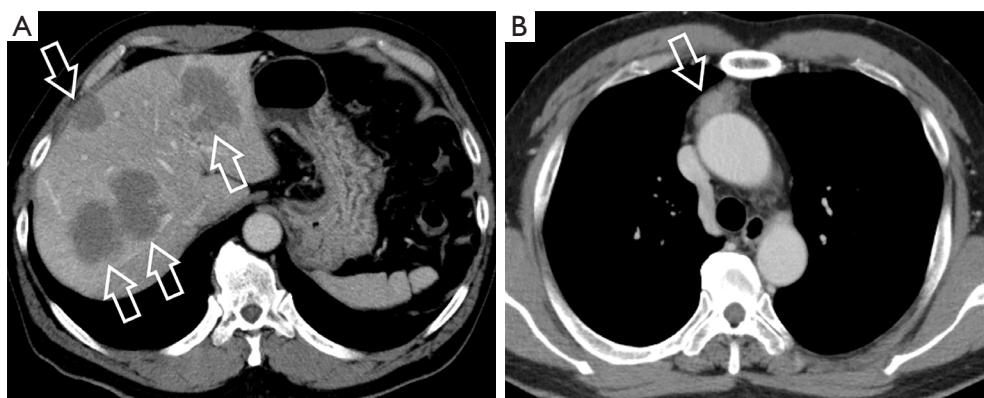


Figure 2 Case 2: a male patient in his fifties, without any noteworthy medical history, was diagnosed with numerous liver neoplasms during a regular health check-up abdominal ultrasound. (A) Contrast-enhanced CT (axial), the liver level; (B) contrast-enhanced CT (axial), the mediastinal level. A CT scan with contrast revealed multiple ill-defined low-density lesions in the liver (A, arrows) and a nodule in the anterior mediastinum (B, arrow). CT, computed tomography.

its slow enlargement, the diagnosis of thymoma was added to the list of differential diagnoses. Additional examination revealed less than 5% of the tumor to be CK5-positive epithelial cells, resulting in a diagnosis of type B1 thymoma that had metastasized to the liver. Chemotherapy was then initiated according to a thymoma protocol. Type B1 thymomas are characterized by a dominance of lymphocytes and may be challenging to differentiate from lymphomas based on histology alone. Importantly, thymomas can metastasize even at low grades [this case was also presented in the reference (31)].

Case 3

A male in his fifties, previously healthy with no significant medical history, presented with an abnormality on chest X-ray during a regular health check-up. Tumor markers such as CYFRA, CEA, NSE, SCC, SLX, GRP, sIL-2R, anti-AChR antibody, were within the normal range. Imaging revealed a well-defined 25 mm nodule in the anterior mediastinum. On plain CT, the lesion appeared hyperdense (*Figure 3A*), and on contrast-enhanced CT, there was enhancement only at the periphery of the lesion (*Figure 3B*).

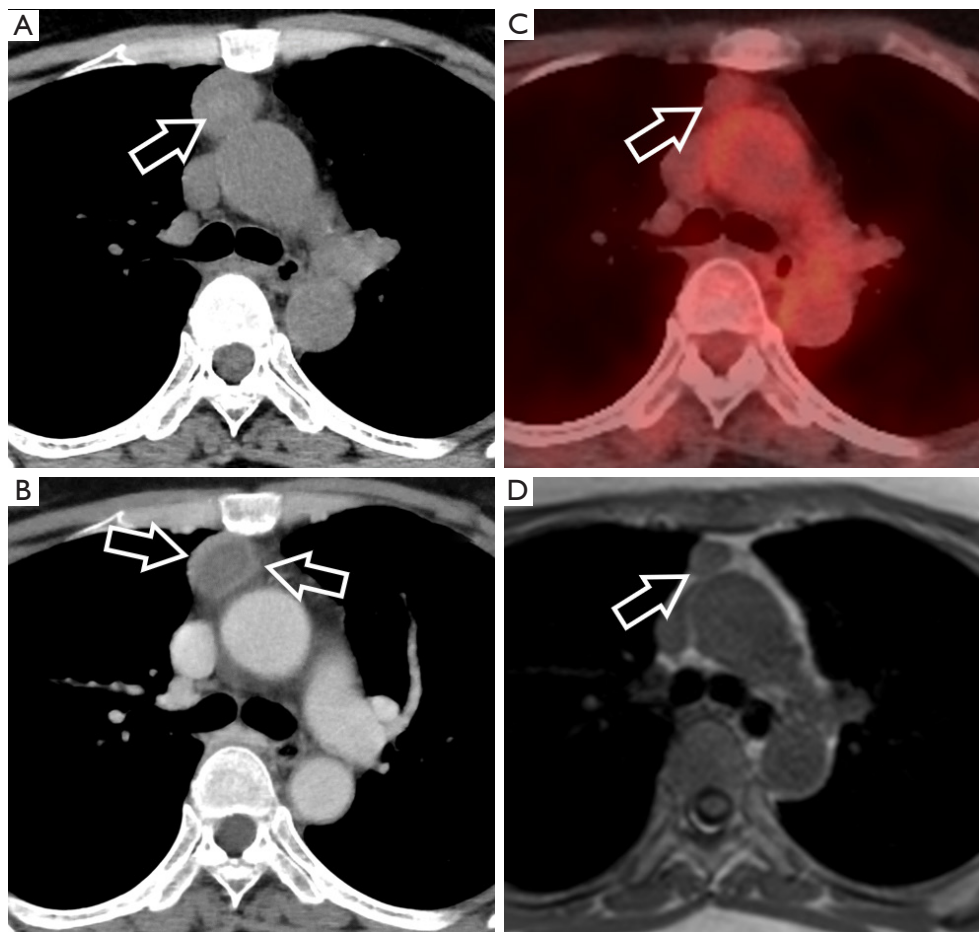


Figure 3 Case 3: a male in his fifties, previously healthy with no significant medical history, presented with an abnormality during a regular health check-up. (A) Plain CT (axial); (B) contrast-enhanced CT (axial); (C) FDG-PET/CT (axial), one and a half month after (A) and (B); (D) T2WI (axial), one and a half month after (A) and (B). The lesion appeared heterogeneously hyperdense in the center before the contrast agent was administered (A, arrow). On contrast-enhanced CT, there was enhancement only at the periphery of the lesion (B, arrows). Imaging performed one and a half months later with MRI and FDG-PET/CT showed a significant spontaneous size reduction from 25 to 15 mm (C,D, arrows). T1-weighted images showed slightly increased signal intensity without fat content. FDG uptake was minimal, but not as low as in cysts. CT, computed tomography; FDG, fluorodeoxyglucose; PET, positron emission tomography; T2WI, T2-weighted images; MRI, magnetic resonance imaging.

Imaging performed one and a half months later with MRI and FDG-PET/CT showed a significant spontaneous size reduction from 25 to 15 mm (Figure 3C,3D). T1-weighted images (T1WI) showed slightly increased signal intensity without fat content. FDG uptake was minimal, but not as low as in cysts. Together with internal hemorrhaging, these imaging findings led to a suspicion of a shrinking solid nodule, predominantly indicative of a thymoma. A thoracoscopic anterior mediastinal tumor resection was subsequently performed, confirming a thymoma B1 with

massive hemorrhage and necrosis. The histopathological results matched the clinical presentation of spontaneous regression, and the lesion was categorized as pT1. This case highlights the significance of not eliminating thymomas from the list of differential diagnoses solely based on initial appearances that may resemble cystic lesions. Even if a lesion appears cystic at first, it is essential to evaluate its internal characteristics through imaging to consider the potential occurrence of a regressing solid nodule, especially concerning thymomas.

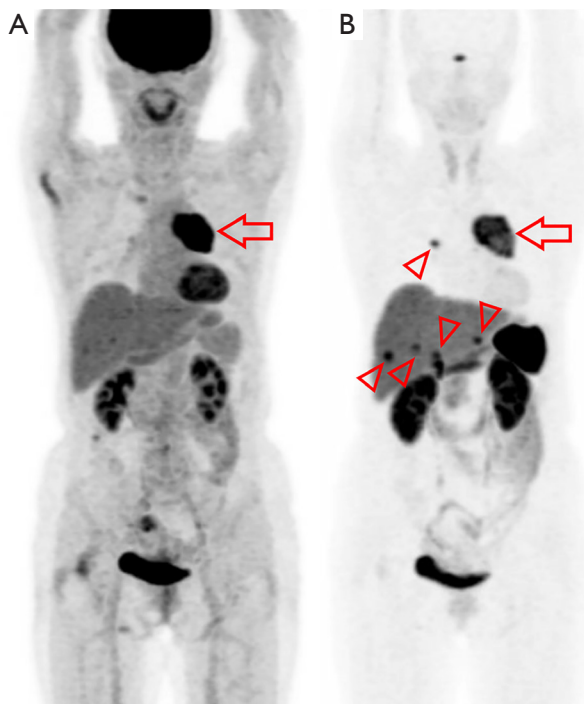


Figure 4 Case 4: a female in her seventies was evaluated by two nuclear medicine examinations. (A) FDG-PET (maximum intensity projection image); (B) ^{68}Ga DOTATOC-PET (maximum intensity projection image). FDG-PET demonstrated intense uptake at the anterior mediastinal mass (A, arrow), albeit without definitive uptake elsewhere. ^{68}Ga -DOTATOC PET revealed intense uptake not only in the anterior mediastinal mass (B, arrow), but also in the right lung hilum and liver, which strongly suggests multiple metastases (B, arrowheads). FDG, fluorodeoxyglucose; PET, positron emission tomography; ^{68}Ga , 68-gallium.

Case 4

A female in her seventies presented with a 6-month history of chest pain radiating from the left neck to the chest. Following evaluation by her primary care physician, a chest X-ray revealed a mass prompting referral to our institution. Given the suspicion of anterior mediastinal tumor, further investigations were pursued. FDG-PET/CT demonstrated intense uptake within the suspected tumor (Figure 4A), albeit without definitive uptake elsewhere. Subsequent ^{68}Ga -DOTATOC PET/CT revealed intense uptake in the anterior mediastinal mass, along with multiple clear accumulations in the right hilar region and liver (Figure 4B). MRI of the liver confirmed metastases (data not shown). Although lung involvement was suspected, histological

confirmation was not performed. Ultrasound-guided biopsy of the anterior mediastinal tumor revealed histopathological features suggestive of squamous epithelial differentiation. Despite initial suspicion of the possibility of primary lung squamous cell carcinoma as well as thymic carcinoma, positivity for CD117, indicative of thymic origin, led to the diagnosis of thymic carcinoma. Neuroendocrine differentiation was absent in hematoxylin and eosin (HE), which was also supported by negative Chromogranin A staining. Given the diagnosis of stage IV thymic carcinoma with multiple hepatic metastases, chemotherapy with ADOC regimen was initiated. However, subsequent emergence of new lesions prompted a shift to best supportive care. In this case, it is evident that the presence of DOTATOC accumulation does not necessarily suggest the possibility of NENs. Particularly in thymic squamous cell carcinoma of thymic origin, where approximately 70% express SSTR2, as reported (45). However, when DOTATOC avidity is observed, lesions can be identified with higher contrast than those revealed by FDG PET, as experienced here.

In addition to the tumors originated from thymus described so far, there are many other neoplastic lesions that require to differentiate from thymoma, which, although less frequent, will be presented in the last section based on case examples.

Case 5

A male in his thirties with no significant medical history was found to have a mediastinal nodule incidentally during a routine health check-up. A contrast-enhanced CT scan showed a well-defined and relatively homogeneous lesion with clear margins (Figure 5). Despite his relatively young age, the nodule's location and characteristics caused suspicion of a thymoma. Consequently, the patient underwent a robot-assisted thymectomy.

The histological analysis revealed a significant enlargement of lymphoid follicles with prominent mantle zones and atrophic germinal centers. Hyalinization was observed in vessels within the follicles. Subsequent immunostaining, comprising CD3, CD20, CD21, Ig kappa [in situ hybridization (ISH)], Ig lambda (ISH), and IRTA1, did not provide any indication of lymphoma or other malignancies. Thus, the conclusive diagnosis was Castleman disease, hyaline vascular type (unicentric Castleman disease). There has been no evidence of recurrence during the 3-year postoperative follow-up. Upon retrospective assessment,

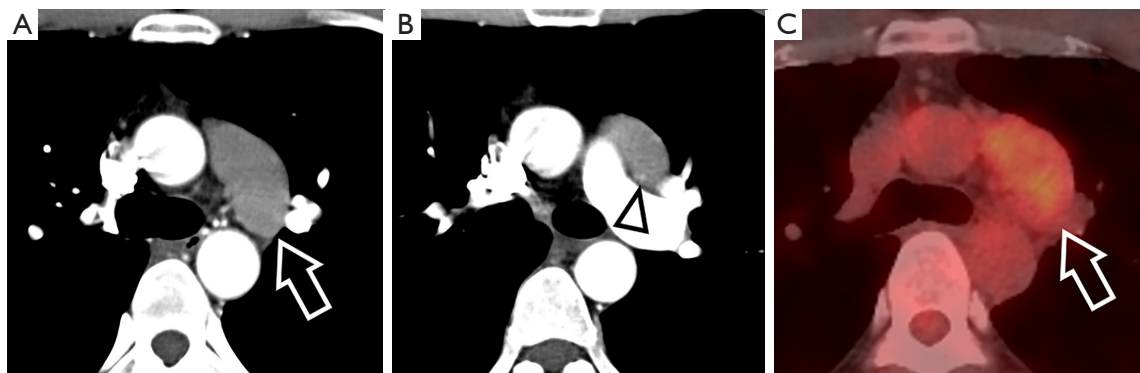


Figure 5 Case 5: a male in his thirties with no significant medical history was found to have a mediastinal nodule incidentally during a routine health check-up. (A,B) Contrast-enhanced CT in the early phase (axial); (C) FDG-PET/CT (axial). Contrast-enhanced imaging showed anterior mediastinal mass lesion (A, arrow) with a relatively prominent feeding vessel at the margins of the mass (B, arrowhead) which was relatively prominent for the size of the lesion. FDG uptake was not intense, but not as low as in cysts (C, arrow). CT, computed tomography; FDG, fluorodeoxyglucose; PET, positron emission tomography.

imaging showed a relatively prominent feeding vessel at the margins of the mass, which was relatively prominent for the size of the lesion and may have been a characteristic finding of Castleman disease. Moreover, the patient's young age was atypical for a thymoma.

Castleman disease, a benign lymphoproliferative disorder, deserves consideration. Castleman disease is thought to be a disease that includes several different etiological conditions. It is classified as unicentric or multicentric, and almost all cases of unicentric Castleman disease are of the hyaline vascular type. Hyaline vascular Castleman disease has distinct pathological features and is considered to be a benign clonal neoplasm derived from lymph node stromal cells, possibly follicular dendritic cells (49). As mediastinal pathology, it often presents as a solitary mass (unicentric) or sometimes multiple lesions (multicentric) in the mediastinum, and its distinction from other mediastinal tumors can be challenging. The disease exhibits characteristic features on imaging, such as early enhancement and dilated feeding vessels in the arterial-dominant phase. Approximately 10% of cases may display branching calcifications within the lesion (50). Preoperative diagnosis may still remain difficult as shown in our case, where Castleman disease was initially suspected as thymoma.

Case 6

A female patient in her fifties complained of hoarseness of one month's duration. Subsequent investigations confirmed left vocal cord paralysis and an upper mediastinal lesion.

Three years ago, a CT scan did not reveal any abnormalities in the upper area of the chest, yet in the current check-up, a 30 mm mass was detected. The contrast-enhanced CT scan showed a lesion with slight enhancement (from 45 HU on the plain scan to 75 HU on the contrast-enhanced scan, *Figure 6A*). In MRI both T1WI and T2WI showed low signal intensity, and FDG uptake was moderate but relatively weak considering the lesion's size (*Figure 6B-6E*). Due to the suspicion of thymoma or a low-grade lymphoma, a biopsy was performed on the mediastinal lesion. Histologically, the specimen exhibited proliferating spindle-shaped cells with eosinophilic cytoplasm. Positive immunostaining was observed for alpha smooth muscle actin (SMA) and beta-catenin (nuclear, focal), while desmin, S-100, CK AE1/AE3, CD34, STAT6, and ALK were all negative. Based on these results and immunostaining, a histological diagnosis of desmoid-type fibromatosis was established. Retrospectively, opposed-phase T1-weighted imaging demonstrated linear low signal intensity within the lesion, suggesting the presence of fat tissue, and the imaging characteristics might raise the possibility of desmoid-type fibromatosis, although it initially mimicked a thymoma.

Desmoid fibromatosis is a fibroblastic neoplasm that exhibits a locally aggressive, non-metastasizing nature with infiltrative growth and a tendency for local recurrence. It is commonly known as aggressive fibromatosis or desmoid tumor. It predominantly develops in the chest wall, although some cases have been reported in the pleura, lung parenchyma and mediastinum. Clinical manifestations may include pain, dyspnea, and kyphoscoliosis. Additionally,

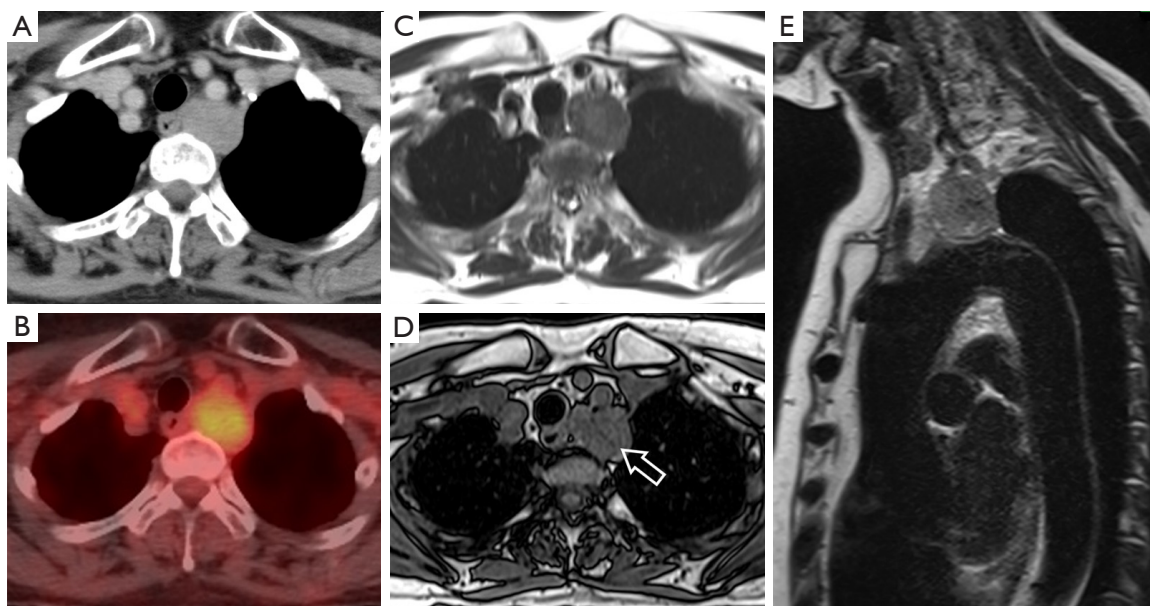


Figure 6 Case 6: a female patient in her fifties complained of hoarseness of 1 month's duration. (A) Contrast-enhanced CT (axial); (B) FDG-PET/CT (axial); (C) T1WI in phase (axial); (D) T1WI opposed phase (axial); (E) T2WI (sagittal). The contrast-enhanced CT scan showed a lesion with slight enhancement (from 45 HU on the plain scan to 75 HU on the contrast-enhanced scan, A). In MRI both T1WI and T2WI showed low signal intensity (C-E), and FDG uptake was moderate but relatively weak considering the lesion's size (B). Note that the opposed-phase T1-weighted imaging demonstrates linear low signal intensity within the lesion (D, arrow), suggesting the presence of fat tissue. CT, computed tomography; FDG, fluorodeoxyglucose; PET, positron emission tomography; T1WI, T1-weighted images; T2WI, T2-weighted images; HU, Hounsfield unit; MRI, magnetic resonance imaging.

it may also be detected incidentally or post-trauma/surgery (51-53). On CT, these tumors are usually well-circumscribed but may show ill-defined margins in more aggressive cases. They appear relatively homogenous or focally hyperattenuating on non-contrast scans, with enhancement following contrast administration. MRI is highly sensitive to local extension caused by its high cellularity. Signal characteristics include low intensity on T1WI and T2WI, and post-contrast T1 images may show variable enhancement patterns. The majority of incidences occur during adulthood and equally affect both genders. Genetic factors, such as somatic mutations in CTNNB1, contribute to the etiology, thereby activating the WNT/ β -catenin pathway. Macroscopically, the lesion manifests as a poorly circumscribed solid mass exhibiting a whorled or trabecular cut surface. Histologically, long sweeping fascicles of fibroblasts infiltrate the surrounding tissue, expressing SMA, muscle specific actin (MSA), and nuclear β -catenin. Diagnosis through cytology from fine needle aspiration (FNA) may prove challenging.

CTNNB1 mutation studies assist in diagnosing cases where morphological characteristics are ambiguous. The prognosis is uncertain, with recurrence rates up to 33%, and margin status inconsistently associated with recurrence risk. Asymptomatic patients may consider a watchful waiting approach (51-53).

Conclusions

Understanding the diagnosis of TETs involves recognizing the classification within the mediastinum, interpreting common imaging findings, and considering differential diagnoses. Here the initial importance of distinguishing between solid and cystic lesions in imaging evaluation has been emphasized. However, differentiation between TETs and other conditions may not always be straightforward based solely on imaging. This review also provides insights into scenarios that may occur in diagnosing TETs and highlights clinically relevant features that enhance imaging diagnosis, illustrated through six case presentations.

Acknowledgments

Funding: None.

Footnote

Provenance and Peer Review: This article was commissioned by the Guest Editor (Masatsugu Hamaji) for the series “Locally Advanced Thymic Epithelial Tumors” published in *Mediastinum*. The article has undergone external peer review.

Peer Review File: Available at <https://med.amegroups.com/article/view/10.21037/med-23-66/prf>

Conflicts of Interest: The author has completed the ICMJE uniform disclosure form (available at <https://med.amegroups.com/article/view/10.21037/med-23-66/coif>). The series “Locally Advanced Thymic Epithelial Tumors” was commissioned by the editorial office without any funding or sponsorship. The author has no other conflicts of interest to declare.

Ethical Statement: The author is accountable for all aspects of the work in ensuring that questions related to the accuracy or integrity of any part of the work are appropriately investigated and resolved. All clinical procedures described in this study were performed in accordance with the ethical standards of the institutional ethical committee of Kyoto University Hospital (No. R2996-1) and with the Helsinki Declaration (as revised in 2013). Written informed consent was obtained from the patients for the publication of this article and accompanying images.

Open Access Statement: This is an Open Access article distributed in accordance with the Creative Commons Attribution-NonCommercial-NoDerivs 4.0 International License (CC BY-NC-ND 4.0), which permits the non-commercial replication and distribution of the article with the strict proviso that no changes or edits are made and the original work is properly cited (including links to both the formal publication through the relevant DOI and the license). See: <https://creativecommons.org/licenses/by-nc-nd/4.0/>.

References

1. Felson B. Chest roentgenology. WB Saunders, Philadelphia; 1973:416-20.
2. Fujimoto K, Hara M, Tomiyama N, et al. Proposal for a new mediastinal compartment classification of transverse plane images according to the Japanese Association for Research on the Thymus (JART) General Rules for the Study of Mediastinal Tumors. *Oncol Rep* 2014;31:565-72.
3. Carter BW, Tomiyama N, Bhora FY, et al. A modern definition of mediastinal compartments. *J Thorac Oncol* 2014;9:S97-101.
4. Carter BW, Benveniste MF, Madan R, et al. ITMIG Classification of Mediastinal Compartments and Multidisciplinary Approach to Mediastinal Masses. *Radiographics* 2017;37:413-36.
5. Nakazono T, Yamaguchi K, Egashira R, et al. CT-based mediastinal compartment classifications and differential diagnosis of mediastinal tumors. *Jpn J Radiol* 2019;37:117-34.
6. Marx A, Detterbeck F, Marom EM, et al. Thymoma: Introduction. In: WHO Classification of Tumours Editorial Board. Thoracic tumours [Internet]. Lyon (France): International Agency for Research on Cancer; 2021 [cited 2023 Dec 1]. (WHO classification of tumours series, 5th ed.; vol. 5). Available online: <https://tumourclassification.iarc.who.int/chapters/35/292>
7. Shah A, Rojas CA. Imaging modalities (MRI, CT, PET/CT), indications, differential diagnosis and imaging characteristics of cystic mediastinal masses: a review. *Mediastinum* 2023;7:3.
8. Ackman JB, Verzosa S, Kovach AE, et al. High rate of unnecessary thymectomy and its cause. Can computed tomography distinguish thymoma, lymphoma, thymic hyperplasia, and thymic cysts? *Eur J Radiol* 2015;84:524-33.
9. Vermoolen MA, Kwee TC, Nievelstein RA. Apparent diffusion coefficient measurements in the differentiation between benign and malignant lesions: a systematic review. *Insights Imaging* 2012;3:395-409.
10. Yacoub JH, Clark JA, Paal EE, et al. Approach to Cystic Lesions in the Abdomen and Pelvis, with Radiologic-Pathologic Correlation. *Radiographics* 2021;41:1368-86.
11. Tateishi U, Müller NL, Johkoh T, et al. Primary mediastinal lymphoma: characteristic features of the various histological subtypes on CT. *J Comput Assist Tomogr* 2004;28:782-9.
12. Tomiyama N, Honda O, Tsubamoto M, et al. Anterior mediastinal tumors: diagnostic accuracy of CT and MRI. *Eur J Radiol* 2009;69:280-8.
13. Perez-Soler R, McLaughlin P, Velasquez WS, et al. Clinical features and results of management of superior

- vena cava syndrome secondary to lymphoma. *J Clin Oncol* 1984;2:260-6.
14. Bayramoğlu Z, Öztürk M, Çalıřkan E, et al. Normative values of thymus in healthy children; stiffness by shear wave elastography. *Diagn Interv Radiol* 2020;26:147-52.
 15. Xia C, Chen S, Baikpour M, et al. Cervical Extension of the Normal Thymus in Children and Adolescents: Sonographic Features and Prevalence. *J Ultrasound Med* 2021;40:2361-7.
 16. Alamdaran SA, Mahdavi Rashed M, Yekta M, et al. Changes in the thymus gland with age: A sonographic evaluation. *Ultrasound* 2023;31:204-11.
 17. Yamazaki M, Yagi T, Ishikawa H. Imaging of Anterior Mediastinal Tumors Other Than Thymic Epithelial Neoplasms. *Japanese Journal of Imaging Diagnosis* 2023;43:165-75.
 18. Ollero García-Agulló D, Martínez de Esteban JP, Toni García M, et al. Tumor-related gynecomastia. *Endocrinol Nutr* 2011;58:554-5.
 19. Nakazono T, Yamaguchi K, Egashira R, et al. Anterior mediastinal lesions: CT and MRI features and differential diagnosis. *Jpn J Radiol* 2021;39:101-17.
 20. Sasaka K, Kurihara Y, Nakajima Y, et al. Spontaneous rupture: a complication of benign mature teratomas of the mediastinum. *AJR Am J Roentgenol* 1998;170:323-8.
 21. Southgate J, Slade PR. Teratodermoid cyst of the mediastinum with pancreatic enzyme secretion. *Thorax* 1982;37:476-7.
 22. Roden AC, Ulbright TM, Marom EM, et al. Germ cell tumours of the mediastinum: Introduction. In: WHO Classification of Tumours Editorial Board. Thoracic tumours [Internet]. Lyon (France): International Agency for Research on Cancer; 2021 [cited 2023 Dec 1]. (WHO classification of tumours series, 5th ed.; vol. 5). Available online: <https://tumourclassification.iarc.who.int/chapters/35/301>
 23. Carter BW, Marom EM, Detterbeck FC. Approaching the patient with an anterior mediastinal mass: a guide for clinicians. *J Thorac Oncol* 2014;9:S102-9.
 24. Mygland A, Vincent A, Newsom-Davis J, et al. Autoantibodies in thymoma-associated myasthenia gravis with myositis or neuromyotonia. *Arch Neurol* 2000;57:527-31.
 25. Arend SM, Dik H, van Dissel JT. Good's syndrome: the association of thymoma and hypogammaglobulinemia. *Clin Infect Dis* 2001;32:323-5.
 26. Lang M, Kazdal D, Mohr I, et al. Differences and similarities of GTF2I mutated thymomas in different Eurasian ethnic groups. *Transl Lung Cancer Res* 2023;12:1842-4.
 27. Masaoka A, Monden Y, Nakahara K, et al. Follow-up study of thymomas with special reference to their clinical stages. *Cancer* 1981;48:2485-92.
 28. Speisky D, de Davila MT, Vigovich F, et al. Hepatic metastasis of thymoma: case report and immunohistochemical study. *Ecancermedicalscience* 2016;10:693.
 29. Vladislav T, Jain RK, Alvarez R, et al. Extrathoracic metastases of thymic origin: a review of 35 cases. *Mod Pathol* 2012;25:370-7.
 30. Martín-Hernández R, Villanueva MM, Sánchez MN, et al. Ovarian Metastasis of a Thymoma: Report of a Case and Literature Review. *Int J Gynecol Pathol* 2015;34:374-8.
 31. Koyasu S. Silent Minority. *Japanese Journal of Imaging Diagnosis*. 2023;43:1187.
 32. Sadohara J, Fujimoto K, Müller NL, et al. Thymic epithelial tumors: comparison of CT and MR imaging findings of low-risk thymomas, high-risk thymomas, and thymic carcinomas. *Eur J Radiol* 2006;60:70-9.
 33. Yabuuchi H, Matsuo Y, Abe K, et al. Anterior mediastinal solid tumours in adults: characterisation using dynamic contrast-enhanced MRI, diffusion-weighted MRI, and FDG-PET/CT. *Clin Radiol* 2015;70:1289-98.
 34. Thuy TM, Duc VT, Vy TT, et al. The value of diffusion-weighted and dynamic contrast-enhanced imaging in the diagnosis of thymic epithelial tumors. *Int J Med Sci* 2022;19:1638-47.
 35. Sung YM, Lee KS, Kim BT, et al. 18F-FDG PET/CT of thymic epithelial tumors: usefulness for distinguishing and staging tumor subgroups. *J Nucl Med* 2006;47:1628-34.
 36. Sharma P, Singhal A, Kumar A, et al. Evaluation of thymic tumors with 18F-FDG PET-CT: a pictorial review. *Acta Radiol* 2013;54:14-21.
 37. Inaoka T, Takahashi K, Mineta M, et al. Thymic hyperplasia and thymus gland tumors: differentiation with chemical shift MR imaging. *Radiology* 2007;243:869-76.
 38. Chan JKC, Marx A, Detterbeck F, et al. Thymic carcinoma: Introduction. In: WHO Classification of Tumours Editorial Board. Thoracic tumours [Internet]. Lyon (France): International Agency for Research on Cancer; 2021 [cited 2023 Dec 1]. (WHO classification of tumours series, 5th ed.; vol. 5). Available online: <https://tumourclassification.iarc.who.int/chapters/35/298>
 39. Inoue A, Tomiyama N, Fujimoto K, et al. MR imaging of thymic epithelial tumors: correlation with World Health Organization classification. *Radiat Med* 2006;24:171-81.

40. Koo YH, Lee JW, Park JS, et al. Primary thymic mucinous adenocarcinoma: A case report focusing on radiological findings and review of the literature. *Iran J Radiol* 2020;17:e101725.
41. Hamaji M, Koyasu S, Omasa M, et al. Are volume-dependent parameters in positron emission tomography predictive of postoperative recurrence after resection in patients with thymic carcinoma? *Surg Today* 2021;51:322-6.
42. Ströbel P, Marchevsky AM, Marom EM, et al. Thymic neuroendocrine neoplasms: Introduction. In: WHO Classification of Tumours Editorial Board. Thoracic tumours [Internet]. Lyon (France): International Agency for Research on Cancer; 2021 [cited 2023 Dec 1]. (WHO classification of tumours series, 5th ed.; vol. 5). Available online: <https://tumourclassification.iarc.who.int/chapters/35/300>
43. Strange CD, Ahuja J, Shroff GS, et al. Imaging Evaluation of Thymoma and Thymic Carcinoma. *Front Oncol* 2021;11:810419.
44. Shimamoto A, Ashizawa K, Kido Y, et al. CT and MRI findings of thymic carcinoid. *Br J Radiol* 2017;90:20150341.
45. Roden AC, Rakshit S, Johnson GB, et al. Correlation of Somatostatin Receptor 2 Expression, 68Ga-DOTATATE PET Scan and Octreotide Treatment in Thymic Epithelial Tumors. *Front Oncol* 2022;12:823667.
46. Lang M, Hackert T, Anamaterou C. Long-term effect of everolimus in recurrent thymic neuroendocrine neoplasia. *Clin Endocrinol (Oxf)* 2021;95:744-51.
47. Villalba JA, Haramati A, Garlin M, et al. Intralesional microbleeding in resected thymic cysts indeterminate on imaging. *Mediastinum* 2023;7:13.
48. Ackman JB, Chintanapakdee W, Mendoza DP, et al. Longitudinal CT and MRI Characteristics of Unilocular Thymic Cysts. *Radiology* 2021;301:443-54.
49. Ferry JA. Tumour-like lesions with B-cell predominance, Introduction In: WHO Classification of Tumours Editorial Board. Thoracic tumours [Internet]. Lyon (France): International Agency for Research on Cancer; 2021 [cited 2023 Dec 1]. (WHO classification of tumours series, 5th ed.; vol. 5). Available online: <https://tumourclassification.iarc.who.int/chapters/35/358>
50. Cabral FC, Trotman-Dickenson B, Madan R. Hypervascular mediastinal masses: action points for radiologists. *Eur J Radiol* 2015;84:489-98.
51. Braschi-Amirfarzan M, Keraliya AR, Krajewski KM, et al. Role of Imaging in Management of Desmoid-type Fibromatosis: A Primer for Radiologists. *Radiographics* 2016;36:767-82.
52. Fritchie KJ, van de Rijn M, Crago AM. Desmoid fibromatosis. In: WHO Classification of Tumours Editorial Board. Soft tissue and bone tumours [Internet]. Lyon (France): International Agency for Research on Cancer; 2020 [cited 2023 Dec 1]. (WHO classification of tumours series, 5th ed.; vol. 3). Available online: <https://tumourclassification.iarc.who.int/chaptercontent/33/40>
53. Dacic S, Noguchi M, Fritchie KJ. Desmoid fibromatosis of the thorax. In: WHO Classification of Tumours Editorial Board. Thoracic tumours [Internet]. Lyon (France): International Agency for Research on Cancer; 2021 [cited 2023 Dec 1]. (WHO classification of tumours series, 5th ed.; vol. 5). Available online: <https://tumourclassification.iarc.who.int/chapters/35/182>

doi: 10.21037/med-23-66

Cite this article as: Koyasu S. Imaging of thymic epithelial tumors—a clinical practice review. *Mediastinum* 2024;8:41.